POWER AND HYDROGEN CO-PRODUCTION IN FLEXIBLE "POWDROGEN" PLANTS

This is the post-print manuscript version of the paper published on J. Eng. Gas Turbines Power. Jun 2023, 145(6): 061007

Paper No: GTP-22-1518. Doi: 10.1115/1.4056045

https://asmedigitalcollection.asme.org/gasturbinespower/article/145/6/061007/1148401/Power-and-Hydrogen-Co-Production-in-Flexible

Alessandro de Cataldo[a], Marco Astolfi[a], Paolo Chiesa[a], Stefano Campanari[a], Emanuele Martelli[a], Paolo Silva[a], Stefano Bedogni[b], Luca Ottolina[b], Marco Tappani[c], Matteo C. Romano[a]

[a]Politecnico di Milano, Department of Energy, Milan, Italy
[b]Edison SpA, Milan, Italy
[c]Ansaldo Energia SpA, Genoa, Italy

alessandro.decataldo@polimi.it
marco.astolfi@polimi.it
paolo.chiesa@polimi.it
stefano.campanari@polimi.it
emanuele.martelli@polimi.it
paolo.silva@polimi.it
stefano.bedogni@edison.it
luca.ottolina@edison.it
marco.tappani@ansaldoenergia.com
matteo.romano@polimi.it

ABSTRACT

This study investigates the potential of "Powdrogen" plants for blue hydrogen and decarbonized electric power production, conceived to operate flexibly depending on the electricity price and to increase the capacity factor of the hydrogen production and CO_2 separation units. The hydrogen production is based on fired tubular reforming or auto-thermal reforming technologies with pre-combustion CO_2 capture by a MDEA process. The power island is based on a combined cycle with H_2-fired gas turbine and a triple pressure reheat heat recovery steam generator (HRSG). The analysis considers three main plant operating modes: hydrogen mode (reformer at full load with hydrogen export and combined cycle off) and power mode (reformer at full load with all hydrogen burned in the combined cycle), plus an intermediate polygeneration mode, producing both hydrogen and electricity. The possibility of integrating the HRSG and the reformer heat recovery process to feed a single steam turbine has been explored to allow keeping the steam turbine hot also in hydrogen operating mode. The economic analysis investigates the competitivity of the plant for different operating hours in hydrogen and power modes. Results suggest that these plants are likely to be a viable way to produce flexibly low-carbon hydrogen and electricity following the market demand.

Keywords: Natural gas, Reforming, Hydrogen, Carbon Capture and storage

1. INTRODUCTION

Securing global net zero greenhouse gas emissions by mid-century and keeping global temperature increase within 1.5 degrees is one of the targets of the recent COP 26 agreement in Glasgow 2021 [1], that will require a transition to decarbonized global economy in the next 30 years. Decarbonization of the power sector [2] is one of the main requirements to meet the ambitious targets of cutting carbon dioxide emissions by 45% in the next 10 years [1, 2]. In this context, in addition to massive deployment of renewable power generation, the switch from coal to natural gas power generation is contributing in the decarbonization of the energy sector in the short term [3]. Gas-fired power plants, thanks to the much lower emissions and the higher flexibility compared to coal power plants, are expected to play a fundamental role in next years to providing balancing services to national and transnational transmission grids with high penetration of non-programmable renewable energy sources [4]. To further reduce CO_2 emissions from fossil fuel power plants, Carbon Capture and Storage (CCS) and sustainable hydrogen market [5] should also be deployed. However, the application of CCS in power plants working in the mid-merit market would cause a significant increase of the cost of electricity due to the high capital intensity of CCS and the low-capacity factor [6]. Also, while green hydrogen produced by electrolysis from renewable energies should be preferred in the long-term due to lower emissions when run with renewable electricity [7], blue hydrogen (i.e. hydrogen from steam reforming of natural gas with CCS) can support the initiation of a low carbon hydrogen market [8], contributing to the decarbonization of the transport and, power sector, as well of of high temperature industrial heating and specific industrial processes (e.g. steel and ammonia production) [9].

The purpose of this study is to investigate the potential of new "Powdrogen" polygeneration plants for the production of blue hydrogen and decarbonized dispatchable power, unlocking the possibility of reaching high-capacity factors for the CCS plant, with economic advantages compared to CCS technologies for separated power and hydrogen generation.

Figure 1 depicts the generic block diagram of a Powdrogen plant composed of the following main sections:

- Chemical island: natural gas is converted into a H_2- and CO_2-rich syngas through steam reforming, based on either fired tubular reforming (FTR) with hydrogen-fired furnace or autothermal reforming (ATR), and Water Gas Shift (WGS) reactors. Heat is recovered from different sections to produce steam for different uses: (i) steam reforming, (ii) power generation in a steam cycle and (iii) solvent regeneration in the reboiler of the MDEA section.
- CO_2 separation: low-carbon H_2-based fuel is obtained after CO_2 separation from syngas by chemical absorption with Methyl diethanolamine (MDEA) carbon capture section. H_2-rich syngas can be used as fuel in combined cycle for electricity production or purified and delivered to the market as "blue" hydrogen.
- Combined cycle: the study considers an advanced H-class gas turbine (GT) designed to operate with high hydrogen content fuels (molar fractions >90%). The gas turbine is coupled with a three-pressure and reheat heat recovery steam cycle.
- Hydrogen purification: pressure Swing Adsorption (PSA) unit allows obtaining high purity hydrogen, releasing low pressure off-gas stream used in the FTR burners or in a boiler if reforming is based on ATR.

The heat and mass balances of Powdrogen plants are computed in different operating modes: (i) hydrogen production mode, where the produced hydrogen is totally exported; (ii) power generation mode, where the H_2-rich syngas is burned in the GT and (iii) polygeneration mode, where hydrogen is partly burned in the GT, which operates at part-load, and partly exported as blue hydrogen.

Two levels of integration of the chemical and power islands are investigated and compared: base configuration and integrated configuration. In the base configuration the chemical island and the combined cycle are connected to two different steam turbines. The former works in steady conditions and its operation exclusively depends on the operational constraints of the main reactor. The latter follows the Gas Turbine operation, which is driven by the electricity selling price. The integrated configuration adopts a single steam turbine (red dashed block in Figure 1) that receives the steam generated both in the syngas coolers and in the combined cycle heat recovery steam generator (HRSG). This configuration allows for a reduction of the system complexity but entails larger efficiency penalization when the system switches from power to hydrogen mode because of the part load performance decay of the steam turbine.

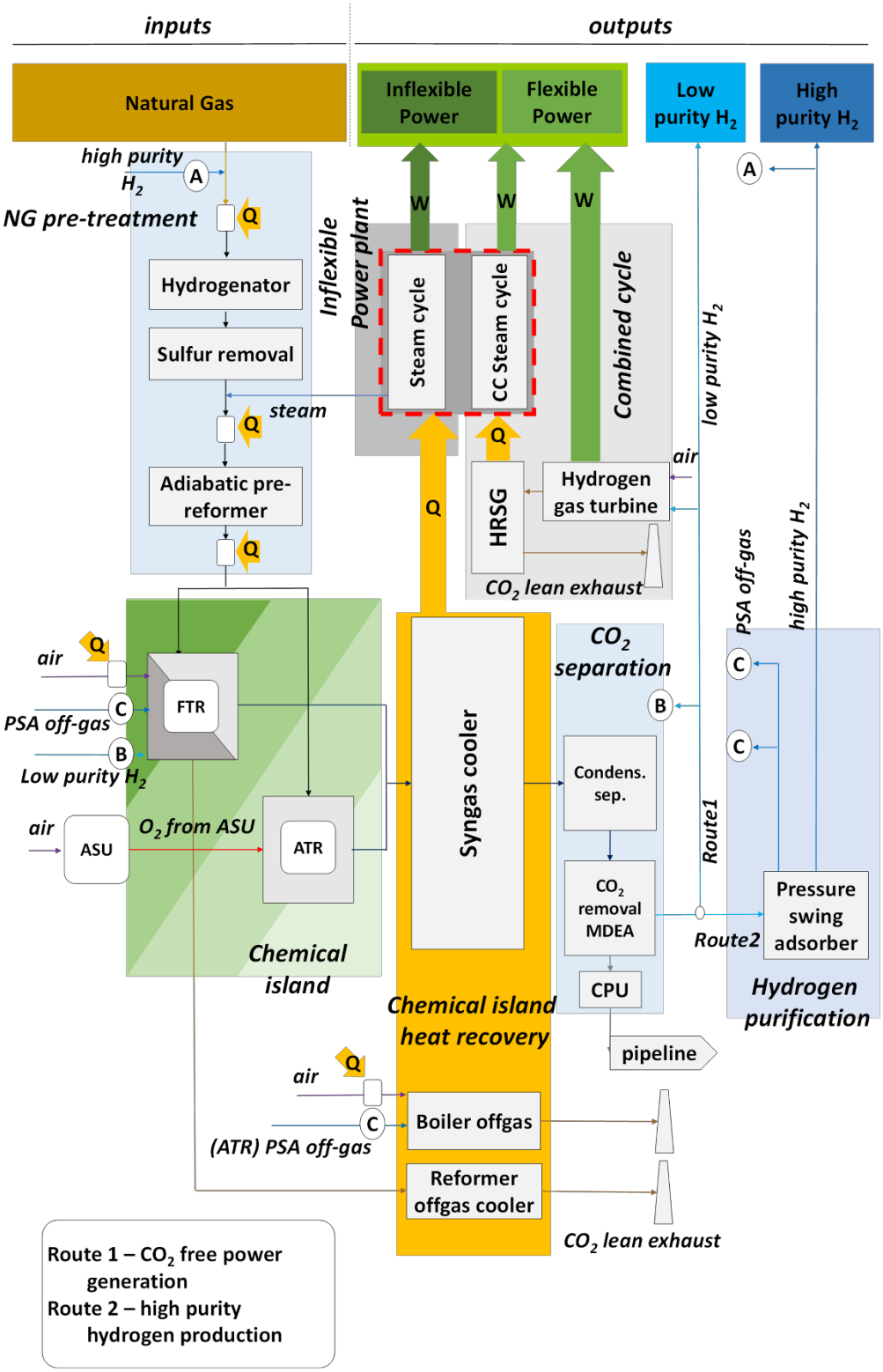

Figure 1: Simplified block flow diagram of a Powdrogen plant

2. PLANT DESCRIPTION

2.1 Steam reforming section

Natural gas contains sulfur compounds which can poison the steam reforming catalyst. According to the best practices of industrial reformers [10], the purification section consists of two steps: organic sulfur in natural gas is hydrogenated by a small amount of recirculated H_2, reaching 2% mol. H_2 in the charge to the hydrogenator [11] to ensure its conversion to H_2S, that is subsequently removed on a zinc oxide (ZnO) bed.

Desulfurized natural gas is then mixed with steam to achieve an adequate steam to carbon ratio (S/C). The preheated charge enters the pre-reformer, in which high hydrocarbons are converted to methane, hydrogen, and carbon monoxide before entering the main reforming reactor. This step is necessary to obtain a homogeneous feedstock composition to the reformer independently of the composition of the primary fuel. The pre-reformer is an adiabatic vessel converting all hydrocarbons that might otherwise react to form unsaturated compounds in the main reformer, leading to carbon deposition.

2.1.1 Fired tubular reforming

Fired tubular reformers employ tubes filled with catalysts placed in a furnace, where heat is transferred by radiation and convection. The tubes are generally 10-14 m long with a diameter between 100-180 mm and a thickness of 8-20 mm [11] and are manufactured with high alloy steels to withstand temperatures of about 1000°C and pressures of about 30 bar. The typical syngas outlet temperature is in the range 800-950°C [12]. Higher temperature can reduce the operative life of the reactor material by inducing accelerated creep. The optimal steam to carbon ratio is in the 2.7-4 range and derives from a trade-off between different effects. Increasing the S/C reduces the energy efficiency of the process because it increases the steam that must be heated in the reformer by burning additional fuel, with little benefits on the hydrogen yield. On the contrary, a low steam to carbon ratio is detrimental for methane conversion and favors carbon deposition that causes an increase of the tube walls temperature with increased thermo-mechanical stresses on the material. Heat for the endothermic reforming reaction is usually provided through the combustion of the PSA off-gas and additional natural gas. In this study, a portion of the produced H_2-rich syngas is used as fuel in the FTR furnace instead of natural gas, in order to reduce CO_2 emissions. The exhausts from the furnace leave the reforming section at 1100°C and are cooled down to 105 °C by preheating the charge to reformer and the combustion air.

2.1.2 Auto-thermal reforming

Auto-thermal reformers encompass two main reaction stages: (i) combustion and (ii) methane reforming. The former consists in the partial oxidation of a fraction of the feedstock and takes place in the burner and the combustion chamber section of the reactor. Partial oxidation occurs with sub-stoichiometric air to fuel ratio, with oxygen to hydrocarbon molar ratio of 0.55-0.6 [13]. In the second stage, methane reforming and WGS are promoted by a catalytic bed separated from the combustion chamber by ceramic plates to protect it from the radiant heat of the flame and overtemperatures. The reactor is contained in a refractory-lined pressure shell and can be considered virtually adiabatic. Temperatures of about 2500°C are reached in the flame core in the combustion zone [13] and about 1100-1300 °C at the inlet of the catalysts bed. The syngas exit temperature is between 800 and 1100 °C. An air separation unit (ASU) is necessary to supply pure oxygen to the reformer to avoid syngas contamination with N_2 that would lead to oversize the PSA unit.

2.2 Syngas conditioning and hydrogen purification

The gas leaves the reformer at high temperature with a high carbon monoxide content [10]. Hydrogen production is substantially enhanced by achieving the equilibrium of the WGS reaction at lower temperature. The WGS section is composed of two adiabatic reactors: the high temperature water gas shift (HT-WGS, using an iron-based catalyst [14]) and the low temperature one (LT-WGS).

The heat available from syngas cooling is recovered to produce steam. The syngas cooling section must be designed considering the risk of metal dusting (i.e. the corrosion phenomena induced by CO-rich gases in the temperature range 400-800°C [11]). To minimize the risk of metal dusting, an evaporator is placed immediately downstream the hot reactor outlet to keep the tube wall temperature below 400°C.

CO_2 separation is performed through absorption with methyl diethanolamine (MDEA) after syngas cooling and condensed water separation. MDEA solvent exhibits an intermediate behavior between chemical and physical solvents, and it is therefore preferred for intermediate values of CO_2 partial pressure like in a pre-combustion capture from natural gas. The MDEA section is simulated as a separator with a CO_2 separation efficiency of 95% and heat demand of 1 MJ/kg of captured CO_2 [15-17]. Heat is supplied by condensing steam at 2 bar, extracted from the chemical island steam cycle.

The separated carbon dioxide is dehydrated and compressed to 110 bar and 28°C to be transported and stored as supercritical fluid [18]. The CO_2 dehydration and compression section includes a train of five intercooled compressors taking the

pressure to 89 bar with an intermediate dehydration section for H_2O removal operated at 15 bar. After CO_2 liquefaction at 89 bar, a pump takes the stream to the final delivery pressure of 110 bar.

Pressure swing adsorption is the state-of-the-art technology for hydrogen purification, that offers the possibility to obtain hydrogen with 99.999% purity, [14, 19-20] with a recovery of about 90%. The low-pressure off-gas containing unconverted CH_4,CO, CO_2, N_2 and unrecovered H_2 is burned either in the FTR furnace or in a boiler in the ATR-based plant. The main process parameters are resumed in Table 1.

Table 1: Main design parameters of the Powdrogen plant

NATURAL GAS DESULPHURIZATION		
Sulphur absorption temperature [°C]	365	
H_2 fraction needed in the charge [% mol]	2	
PRE-REFORMING	FTR	ATR
S/C ratio	3.4	1.5
Inlet temperature [°C]	490	490
ASU		
Electric consumption [kWh/tonO_2]	-	300
O_2 delivery pressure [bar]	-	40
O_2 purity [%mol.]	-	95
REFORMER		
Exit temperature [°C]	890	1050
Exit pressure [bar]	32.7	32.7
Heat losses [% of fuel LHV input in the furnace]	0.2	-
WGS REACTOR		
HT-WGS inlet temperature [°C]	340	340
LT-WGS inlet temperature [°C]	195	210
MDEA SECTION		
CO_2 separation efficiency [%]	95	
Reboiler heat duty [MJ/kgCO_2]	1	
CO_2 COMPRESSOR		
Compressor outlet pressure [bar]	110	
IC compressor isentropic efficiency [%]	84	
IC comp. mech-electric efficiency [%]	94	
Pump efficiency [%]	80	
Intercooler outlet temperature [°C]	35	
PSA		
H_2 recovery efficiency [%]	89	
Off-gas pressure [bar]	1.3	
PRESSURE LOSSES		
Gas side pressure loss in heat exc. [%]	2	
Pressure loss in pre-reformer [bar]	1	
Pressure loss in reformer [bar]	2.4	

2.3 Power island

The chemical island is sized to supply H_2-rich syngas to a H-class gas turbine, with nominal power output of 536 MW_e when fired with natural gas and combined cycle efficiency of around 63%. Combined Cycle performance has been evaluated under the assumption that the gas turbine can burn high hydrogen (>90% vol.) fuel in a premixed combustor without any significant change in the design parameters compared to the corresponding natural gas fired conditions, representing a design target shared by most current GT manufacturers. Two cases have been considered for the design of the heat recovery steam cycle: (i) non-integrated design, where two different steam turbines are adopted for the steam generated in the HRSG of the combined cycle and the steam generated in the chemical island and (ii) integrated design, where a single steam turbine

is used for both the sources of steam (Figure 2). The integrated solution allows keeping the steam turbine hot when the plant runs in hydrogen mode (i.e. when the gas turbine is off). Differently from the non-integrated design, the integrated configuration requires the introduction of a reheating section into the chemical island, so that reheated steam (RH) is produced also when the GT is off. Temperature and pressure of the steam from the chemical island are the same of the HRSG. This configuration has the disadvantage that the steam turbine experiences very different steam flow rates between operations in power mode (design condition for the steam turbine) and hydrogen mode.

Table 2 depicts the main parameters of the steam cycles of the combined cycle and the chemical island. The condenser is sized to operate at a design pressure of 0.04 bar. While the minimum operating pressure has been assumed to be 0.025 bar.

Table 2: Steam cycles design specifications

CHEMICAL ISLAND STEAM CYCLE (non-integrated case)	
HPT inlet temperature [°C]	540
HPT inlet pressure [bar]	100
Design condensing pressure [bar]	0.04
Minimum operating condensing pressure [bar]	0.025
HRSG STEAM CYCLE	
HPT temperature non-integrated/integrated [°C]	600/560
HPT/IPT/LPT inlet pressure [bar]	160/36/6
Design condensing pressure [bar]	0.04
Minimum condensing pressure [bar]	0.025

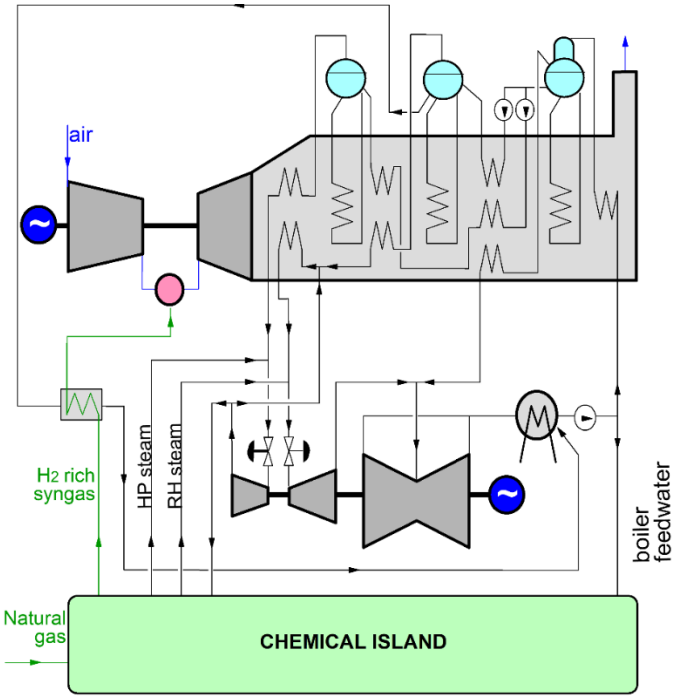

Figure 2: Simplified process flow diagram of the integrated steam cycle

2.4 Operating modes

To assess the operational flexibility of the Powdrogen plant, the following operating modes have been considered:

- Hydrogen mode: the plant receives natural gas and produces hydrogen as main output, operating the chemical island section at full load. An additional relatively small power output is generated by the chemical island heat recovery

steam cycle that exploits heat from syngas and exhaust gas cooling. The gas turbine is off. This is the nominal operating mode for the Powdrogen plant, that defines the design specifications of the process units, of the heat exchangers in the chemical island and of the chemical island steam cycle in the non-integrated configuration.

- Power mode: the chemical island works at full load and all the H_2-rich syngas produced is burned in the gas turbine. The only output from the plant is electricity since no hydrogen is exported. For this reason, the PSA is switched off in power mode. Given the size of the selected gas turbine, this operating mode sets the capacity of the chemical island, i.e. the maximum syngas flowrate produced at full load for both power and hydrogen mode.
- Polygeneration mode: the plant produces both hydrogen and electricity. The chemical island operates at full load, part of the syngas produced is burned in the combined cycle which works at minimum load and the remaining syngas is sent to the PSA for co-production of high purity hydrogen.

3. MODEL

The chemical island of all plants was simulated with Aspen Plus process simulation software [21]. The thermodynamic model used to simulate the systems is the Non-Random Two Liquids modl [22] which is an activity-coefficient model used to describe mixtures far from ideal with the Redlich-Kwong equation of state (NRTL-RK [23]), which describes the vapor phase property for non-ideal mixtures. The NRTL-RK model is one of the most widely used and it is particularly useful when dealing with mixtures phase equilibria.

Aspen Plus was also used for the nominal and off-design characterization of the components of both the chemical island steam cycle and the combined cycle steam power plant. All chemical reactors are calculated at chemical equilibrium, considering CH_4 as an inert in the WGS reactors.

The H_2-fired gas turbine has been calculated with in-house GS code [24] with the cooled gas turbine model [25, 26] calibrated on Ansaldo GT data.

3.1 Off-design model

Once the surface area of the heat exchangers is computed in design mode, the off-design operating modes are calculated by assuming that the heat transfer coefficient is function of the fluid mass flow rate according to Equation (1). The overall heat transfer coefficient is then derived by Equation (2), with the assumption that the conductive resistance of the heat exchanger tubes is negligible.

$$h_{off} = h_{des} \cdot \left(\frac{\dot{m}_{off}}{\dot{m}_{des}}\right)^{0.8} \quad (1)$$

$$U = \left(\frac{1}{h_{HOT}} + \frac{1}{h_{COLD}}\right)^{-1} \left[\frac{\mathrm{W}}{\mathrm{m^2K}}\right] \quad (2)$$

The chemical island steam cycle operates under the assumption of constant evaporation pressure, to reduce the variation of the temperature profiles in the different operating modes and keep the syngas temperature at the inlet of the WGS reactors stable. For the same reason, also the steam reheating pressure is kept constant by a throttling valve in the integrated steam cycle configurations.

Throttling admission valves are used to control the high-pressure and intermediate-pressure steam turbines. The HP turbine operates with a fixed outlet pressure, as steam is extracted at fixed pressure to be mixed with natural gas before the reforming process. The isentropic efficiency is calculated with routines to simulate off-design conditions [27, 28].

The condenser is simulated by assuming constant cooling water flow rate and temperature, leading to a condensation pressure reduction at partial loads.

The heat and mass balances for the gas turbine at minimum load derive from Ansaldo data.

The chemical island can be operated at reduced load, assuming a maximum turn-down rate of 50% (i.e. 50% of NG input to the reformer [29]). The main assumptions for off-design operation are that the PSA, the MDEA section, the ASU and all the reactors are operated in the same conditions as in nominal operation. More specifically: (i) H_2 recovery of the PSA, (ii) CO_2 separation efficiency and specific heat duty of the MDEA process, (iii) specific electric consumption per unit of O_2 produced in the ASU, (iv) chemical equilibrium composition at the exit of the reactors and (v) hot gas temperature at

the reformer furnace outlet is assumed not to change in off-design operations. Referring to the three considered operating modes, the only difference in operation is experienced by the PSA unit that is switched off in power mode and works at reduced load in polygeneration mode.

4. TECHNICAL RESULTS

The technological solutions are evaluated on the basis of the following key performance indexes.

- The hydrogen production efficiency measures the ratio between the heating value output exported as hydrogen over the heating value of the natural gas input, according to Equation (3).

$$\eta_{H2} = \frac{\dot{m}_{H2} \cdot LHV_{H2}}{\dot{m}_{NG} \cdot LHV_{NG}} \quad (3)$$

- The equivalent H_2 production efficiency (Equation (4)) considers the "equivalent" natural gas input, including the credits from electric power export $\dot{P}_{el}$, accounted by assuming a reference combined cycle efficiency of 63%.

$$\eta_{H2\_eq} = \frac{\dot{m}_{H2} \cdot LHV_{H2}}{\dot{m}_{NG} \cdot LHV_{NG} - \frac{\dot{P}_{el}}{\eta_{el,ref,NGCC}}} \quad (4)$$

- The net electric efficiency (Equation (5)) measures the ratio between the net electric output over the heating value of the natural gas input.

$$\eta_{el} = \frac{\dot{P}_{el}}{\dot{m}_{NG} \cdot LHV_{NG}} \quad (5)$$

- The specific CO_2 emission can be calculated referring to hydrogen (Equation (6)) or power (Equation (7)) output, depending on the operation mode. The specific emission considers the CO_2 mass flow rate directly emitted by the plant at the stack.

$$E_{H2} = \frac{\dot{m}_{CO2\_emitted}}{\dot{m}_{H2} \cdot LHV_{H2}} \left[\frac{g_{CO2}}{MJ_{H2}}\right] \quad (6)$$

$$E_{El} = \frac{\dot{m}_{CO2\_emitted}}{\dot{P}_{el}} \left[\frac{kg_{CO2}}{MWh_{el}}\right] \quad (7)$$

- The carbon capture ratio (CCR) is defined as the molar ratio between the captured carbon (as CO_2) and the carbon entering with natural gas as described in Equation (8).

$$CCR = \frac{\dot{n}_{C,stored}}{\dot{n}_{C,GN}} \quad (8)$$

- The Specific Primary Energy Consumption for CO_2 Avoided **(**SPECCA [30]) represents the energy consumption associated to a unit of CO_2 emission avoidance.
  In Hydrogen mode (Equation (9)), it is defined as the ratio between the differences in specific equivalent fuel consumption ($1/\eta_{H2,eq}$) and equivalent CO_2 emission with reference to a Fired Tubular Reformer plant without CCS (i.e. $\eta_{H2,eq,ref}$ = 79.7%, $E_{H2,eq,ref}$ = 73.4 g_{CO2}/MJ_{H2}).
  In Power mode (Equation (10)), it is defined as the ratio between the variations of heat rate ($3600/\eta_{el}$) and CO_2 emission with reference to a natural gas combined cycle without CCS ($\eta_{el,ref}$ = 63%, $E_{el,ref}$ = 325.6 $kgCO_2/MWh$).

$$SPECCA = \frac{\frac{1}{\eta_{H2,eq}} - \frac{1}{\eta_{H2,eq,ref}}}{E_{H2,ref} - E_{H2}} \left[\frac{MJ_{LHV}}{kg_{CO2}}\right] \quad (9)$$

$$SPECCA = \frac{\frac{3600}{\eta_{el}} - \frac{3600}{\eta_{el,ref}}}{E_{el,ref} - E_{el}} \left[\frac{MJ_{LHV}}{kg_{CO2}}\right] \quad (10)$$

4.1 Results

Table 3 depicts the performance of the four assessed plants (FTR and ATR with non-integrated and integrated "I" steam cycle) in hydrogen mode. The Fired tubular reformer (FTR) configuration has a 74.6% H_2 production efficiency (η_{H2}), slightly higher than the auto-thermal reformer (ATR) that achieves 73.1%. The integrated configurations show similar hydrogen production efficiencies, but lower equivalent production efficiencies. The slightly lower hydrogen production for the FTR-I is due to the lower steam temperature at the HP turbine outlet. A fraction of this steam is mixed to natural gas to originate the reforming charge. As the steam temperature in the charge decreases, more syngas is burned in the furnace to keep the same reformer outlet temperature. At constant input charge flow rate, an increase in the syngas flow rate to the furnace brings about a reduction of the H_2 output flow rate. In terms of CO_2 emissions, the ATR achieves significantly lower emissions (0.9-1.0 kg_{CO2}/kg_{H2}, vs. 1.9 kg_{CO2}/kg_{H2}), resulting from higher CO_2 capture efficiency (about 90% vs. 79%). SPECCA varies in the range 0.98-1.46 MJ/kg_{CO2} and 1.2-1.3 MJ/kg_{CO2} for FTR- and ATR-based plants respectively. The higher variation in the FTR-based plants is related to the higher drop of power generated (reflecting in a drop of 1.6% points of equivalent H_2 efficiency) of the integrated steam cycle case (FTR-I-H), caused by the strong reduction of steam flow rate in hydrogen mode, as discussed further on.

Table 3: Performance data of FTR and ATR-based plants with non-integrated and integrated (I) steam cycles in hydrogen mode

	FTR-H	ATR-H	FTR-I-H	ATR-I-H
NG thermal input, MW	1692	1419	1693	1419
Hydrogen output, MW	1262	1038	1254	1039
Net electric output, MW	23.08	21.85	8.62	17.25
H_2 prod. efficiency, %	74.59	73.13	74.10	73.21
Eq. H_2 prod. effic., %	76.24	74.98	74.67	74.66
Carbon capture ratio, %	78.88	89.27	78.85	90.14
Spec. emiss, g_{CO2}/MJ_{H2}	16.16	8.37	16.29	7.68
Spec. emiss, kg_{CO2}/kg_{H2}	1.94	1.00	1.95	0.92
SPECCA, $MJ/kgCO_2$	0.98	1.20	1.46	1.28

Table 4 shows the performance of Powdrogen plants in power mode. The ATR-based plant shows the highest net electric efficiency ($\eta_{el} = 51.3\%$), 2.1% points higher than the FTR, which showed a higher H_2 production efficiency in hydrogen mode. The reason of this result is that in hydrogen mode the FTR configuration makes a better use of the chemical energy in the PSA off-gas stream, that is burned in the FTR burners. Conversely, in the ATR-based plants, the PSA off gas is burned in a boiler when operating in hydrogen mode (thus converted with lower efficiency).

In power mode, all the syngas from the chemical island of the ATR plant is supplied to the combined cycle. Conversely, in the FTR plant, part of the H_2-rich fuel is combusted as low-carbon fuel in the FTR burners. For this reason, the FTR consumes a higher amount of natural gas (+20%) to produce the H_2-rich fuel for a gas turbine of given size.

Table 4: Plant performance data in power mode

	FTR-E	ATR-E	FTR-I-E	ATR-I-E
NG thermal input, MW	1692	1419	1693	1419
Net power output, MW	831.4	727.4	821.3	717.5
Net electric efficiency, %	49.14	51.25	48.54	50.56
Carbon capture ratio, %	78.51	89.23	78.73	89.89
Spec. emiss., kg_{CO2}/MWh_{el}	90.46	43.42	90.32	41.34
SPECCA, $MJ/kgCO_2$	6.85	4.64	7.24	4.95

Table 4 also shows that configurations with integrated steam cycle present a small reduction (-0.60% points for FTR and -0.69% for ATR) in electrical efficiency compared to the non-integrated plants due to the constraints imposed on steam turbine to allow low load operations in hydrogen mode.

In the integrated solutions (ATR-I and FTR-I), the same turbine expands the steam generated in both the chemical island and the HRSG of the combined cycle, thus requiring a single, larger steam turbine. The integrated configurations have the main advantage of keeping the steam turbine of the combined cycle hot in H_2-mode operation, limiting the startup time of the combined cycle when the gas turbine is switched on. Moreover, adopting a single turbine reduces the capital expenditures related to the steam cycle. On the other hand, the integrated steam cycle involves that the steam cycle operates with much lower steam flow rates when switching from power mode to hydrogen mode because, in the latter case, only the steam from chemical island is available. This leads to: (i) a limited turn-down ratio of the reformer when operated in hydrogen mode, limit set by minimum acceptable flow rate for a correct operation of the low-pressure turbine and (ii) efficiency losses at nominal point caused by the sub-optimal steam turbine design (i.e., decreased inlet temperature to HPT due to the lower SH steam temperature from syngas cooling section; reduced blade length of the LP turbine last stage (46 inches vs. 43 inches of the FTR-I configuration) to prevent ventilation losses), required to extend the operating range towards low loads in hydrogen mode. This effect is more pronounced in the FTR-based plant, that operates with 16.5% of the steam flow rate at the LP turbine exit, vs. 33.5% of the ATR plant. The main differences in the process parameters of the steam turbines of the plants with integrated steam cycle are summarized in Table 5.

Table 5: Steam turbine integrated configuration

POWER MODE	FTR-I	ATR-I
Steam inlet to HPT, kg/s	266.2	197.0
Inlet temperature to HPT, °C	560	560
Live steam pressure, bar	150	150
Outlet mass flow from LPT, kg/s	173.5	153.0
HYDROGEN MODE	FTR-I	ATR-I
Steam from chemical island, kg/s	155.4	124.5
Inlet temperature to HPT, °C	470.0	540.5
Live steam pressure, bar	150	150
Pressure after throttling valve, bar	82.79	94.42
Outlet mass flow from LPT, kg/s	28.62	51.32
LP mass flow rate, % of power mode	16.5	33.5

The plants with non-integrated steam cycles were simulated also in polygeneration mode. Results are reported as depicted in Table 6, simulated by assuming that the chemical island operates at full load while the gas turbine of the combined cycle runs at minimum load.

Table 6: Plant performance data in Polygeneration mode

	FTR-Pol	ATR-Pol
Natural gas thermal input, MW	1692	1419
Hydrogen output, MW	682.6	565.4
Net electric plant output, MW	336.9	287.16
Chemical island electric balance, MW	23.86	-11.20
H_2 production efficiency, %	40.34	39.84
Net electric efficiency, %	19.91	20.23

Operating maps of the Powdrogen plants based on FTR (upper chart) and ATR (lower chart) in non-integrated mode are shown in Figure 3. The map shows the region of hydrogen and electricity outputs in which the plant can operate.

Vertices of the region represent one of the calculated operating modes. Points H and MH represent the hydrogen mode operating points, where the plant operates as a merchant H_2 plant and can tune H_2 output from nominal load (H) to minimum load (MH), assumed equal to 50% of the reformer capacity. Point E identifies the power mode, where steam reformer and combined cycle run at full load and no hydrogen is exported from the plant. In the polygeneration point (Pol), the reformer works at nominal condition, while the GT operates at minimum load and about 54% of the nominal hydrogen output is exported. Point MPol identifies the case in which the reformer operates at minimum load and the GT runs at minimum load, involving a small hydrogen output. Moving from point Pol to point MPol, the electric power output decreases in the FTR plant because the effect of the reduced steam turbine power output prevails. The same effect is less pronounced for the ATR plant, due to the reduced consumption for O_2 production. Finally, ME refers to the operating point with the reformer at minimum load and no hydrogen export, resulting in a higher GT load with respect to MPol. The charts also show the Carbon Capture Ratio (CCR) at each simulated operating point.

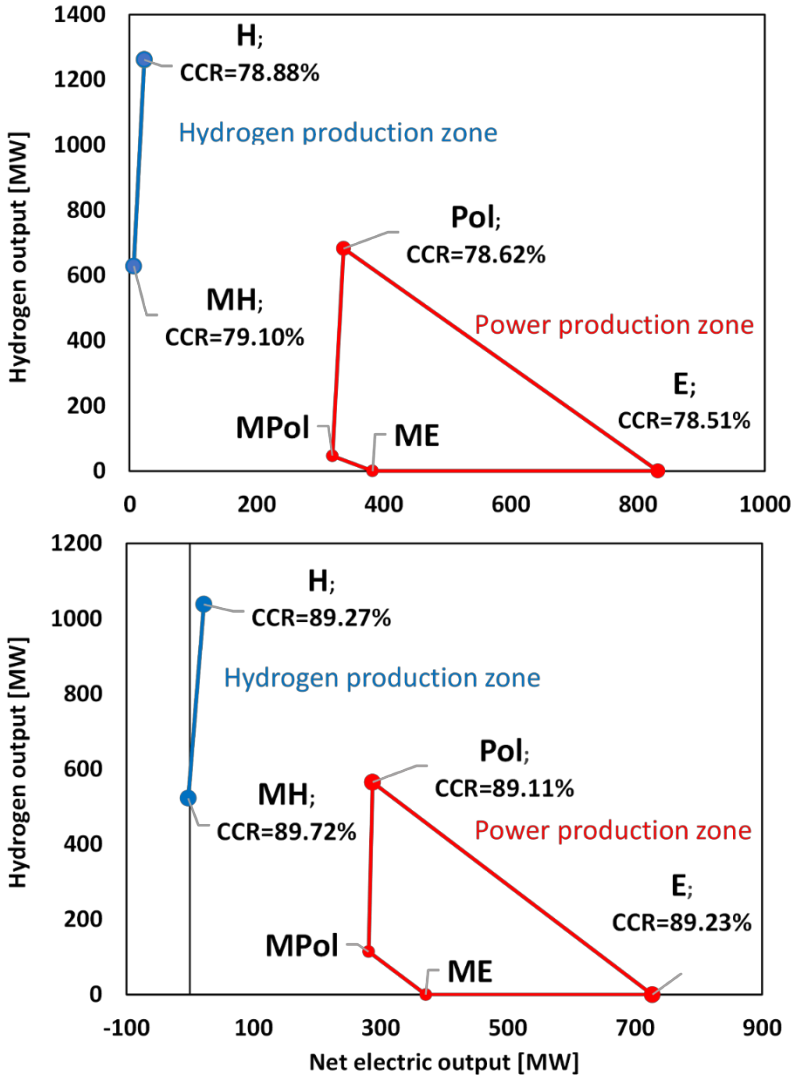

Figure 3: Operating map for the FTR- (top chart) and ATR-based (bottom chart) Powdrogen plants (non-integrated mode)

5. ECONOMIC ANALYSIS

An economic analysis has been carried out for the plants with non-integrated steam cycle, following the procedure in [31] and using data from literature and previous works to estimate the Total Plant Costs (TPC) and the Total Capital Requirements (TCR). The costs for each section of the plants are mostly retrieved from [31, 32] adjusted to 2020 through the CEPCI index [33] and scaled to the proper size thanks to the exponential law (Equation (11)). Total Capital Requirements include spare parts, start-up costs, owner's cost, interest during construction and working capital as described in [31].

$$C = C_{ref}\left(\frac{P}{P_{ref}}\right)^{f} \qquad (11)$$

Breakdown of the Total plant cost of the main units is reported in Table 7, the cost share of the hydrogen production island is lower in the ATR-based plant, mainly because of the lower capacity of the syngas production island needed to produce the syngas to feed the combined cycle. Specific cost data for the assessed plants are shown in Table 8. The "Retrofit" cases refer to the retrofit of an existing combined cycle, whose capital costs are excluded. The ATR-based plants feature the highest absolute and specific total plant costs in all cases. This is due to the scale effect, resulting from the need of a reformer with smaller capacity in the ATR case (340'000 Nm^3/h) with respect to the FTR case (420'000 Nm^3/h made of two parallel trains [10]).

Table 7: Cost breakdown for FTR and ATR H_2 synthesis process

UNIT	FTR [M€]	FTR%	ATR [M€]	ATR%
Air separation unit	-	-	288.4	22.6
Syngas generation	222.6	18.7	95.1	7.5
Hydrogen purification	50.5	4.2	43.3	3.4
Steam turbine and Generator	48.9	4.1	53.9	4.2
Syngas cleanup	64.3	5.4	46.9	3.7
CO_2 Compression and drying	83.9	7.1	74.8	5.9
Feedwater and Miscellaneous BOP systems	199.9	16.8	153.9	12.1
Combined cycle	519.9	43.7	519.9	40.7
Total plant cost	1190		1276	
Total Capital Requirements, M€	1546		1643	

Table 8:Total plant cost and specific total plant cost for the FTR- and ATR-based plants

	New built combined cycle		Retrofit combined cycle	
	FTR	ATR	FTR	ATR
TPC M€	1190	1276	670.2	756.4
Specific TPC €/kW_{el}	1431	1754	806.1	1040
Specific TPC €/$kW_{H2\text{-}exp}$	942	1228	530.6	728.2

As for the operating costs, the main assumptions are related to the cost of natural gas (assumed at 9 €/GJ), cost for CO_2 transport and storage (10 €/t) and carbon tax (100 €/t). The maintenance costs are evaluated as a fixed percentage (1.5%) of Total plant cost per year plus maintenance labour (40% of the overall maintenance cost). The main financial assumptions are given in Table 9.

Table 9: Main financial assumptions

Construction period	3 years
Capital expenditure curve	20/45/35%
Interest during construction	8%
Plant lifetime	25 years
Capacity factor	86%
Inflation	2%
Discount rate	8%
Owner's cost	7%

The Cost of Electricity (COE) and the Cost of hydrogen (COH) (i.e. the breakeven selling prices of electricity and hydrogen) have been evaluated by assuming a discount rate of 8%, an inflation rate of 2%, 25 years of plant lifetime and 7500 equivalent operating hours per year. The study is based on Discounted Cash Flow analysis, depreciation was not considered since the results are reported on the Earnings Before Interest, Taxes, Depreciation and Amortization (EBITDA) basis.

The COE breakdown is shown in Figure 4 for a hypothetical Powdrogen plant that operates always in power mode. The highest share is associated to natural gas, followed by capital expenditures. Capital expenses have a higher impact on the COE for the ATR. For the FTR, the cost associated with the carbon tax is higher compared to ATR, due to the higher specific emissions.

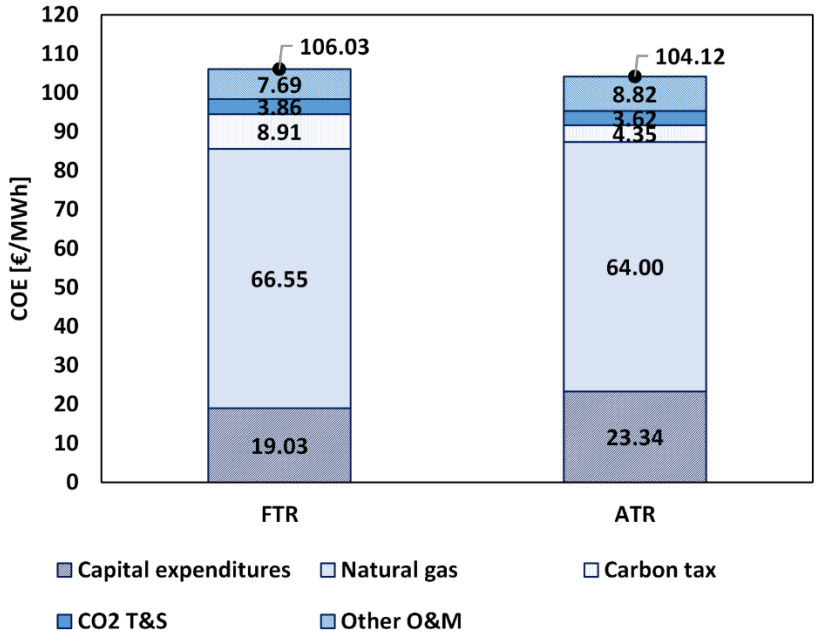

Figure 4: Breakdown of the COE for FTR and ATR plants, assumed to operate always in power mode

The COH breakdown is shown in Figure 5 for two different electric prices (30-70 €/MWh), referring to a hypothetical Powdrogen plant that operates always in hydrogen mode. The ATR has the highest cost of hydrogen and shows the highest incidence of the capital cost expenditures. Both ATR and FTR plants are only slightly sensitive to variation in electricity

prices, which have a limited impact on the COH (negative segments on the figure) given the limited amount of electricity sold (the power output is 21-23 MW vs. 727-831 MW in the power mode).

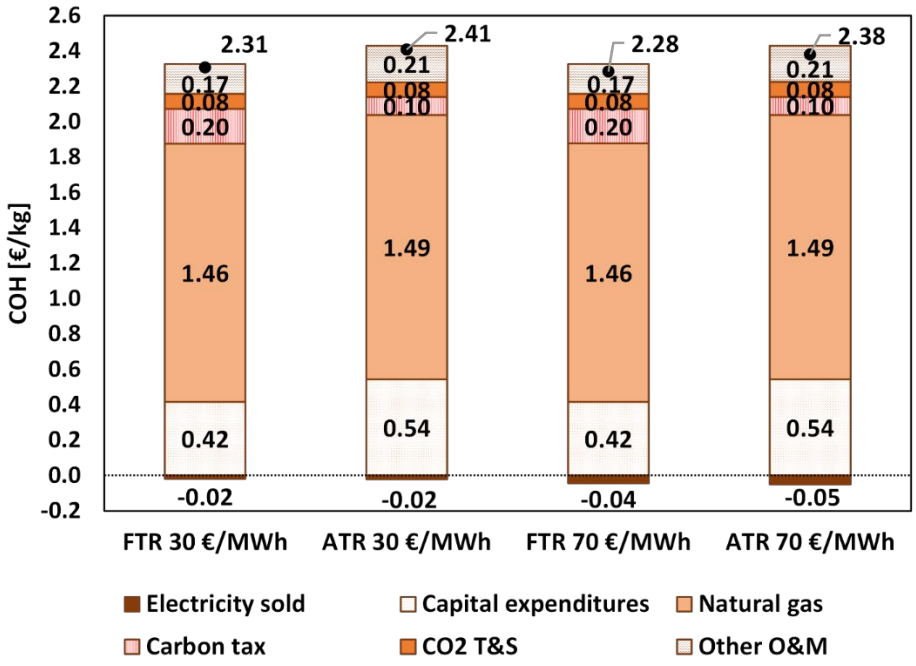

Figure 5: Breakdown of the COH for FTR and ATR plants assumed to operate always in hydrogen mode, for different electricity prices

An analysis on the internal rate of return (IRR) is finally carried out. Each line in Figure 6 shows the iso-IRR=8% curves with the selected value as a function of the electricity and hydrogen selling prices. If the point of the average selling prices of hydrogen and electricity is higher than the values of the curve, then the plant is profitable (i.e. its IRR is higher than 8%). The lines refer to FTR and ATR plants with three different shares of operating modes, from a hydrogen-prevalent (75% hydrogen mode – 25% power mode) to a power-prevalent (25% hydrogen mode – 75% power mode) production regime. The FTR plant shows higher competitivity if operated primarily in hydrogen mode, while the ATR appears to be the equally profitable if operated mainly in power mode.

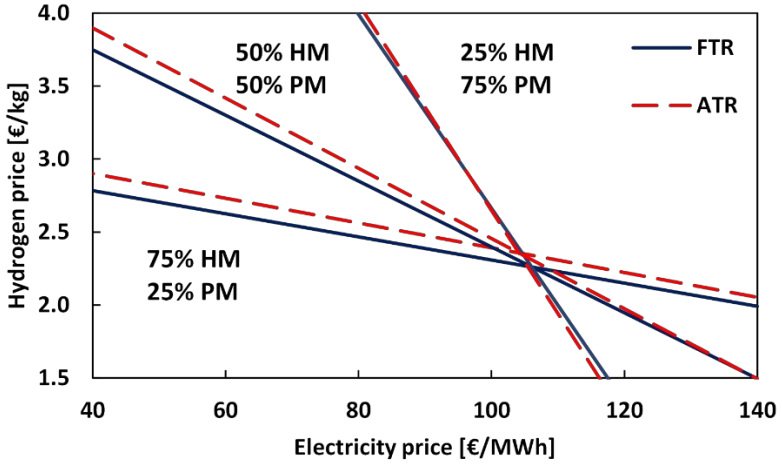

Figure 6: Iso-IRR (IRR=8%) curves for the FTR and ATR plants in three different shares of operating modes

6. CONCLUSION

This study investigated the potential of “Powdrogen” plants for the production of decarbonized electric power and blue hydrogen from natural gas, based on a hydrogen production plant using FTR or ATR connected to a H-class combined cycle, able to operate flexibly depending on the electricity price, while keeping a high-capacity factor of the hydrogen production and CO_2 separation units. Different configurations for the steam cycle (single steam turbine for the steam from the chemical island and the combined cycle vs. two separate steam turbines) and different operating modes (hydrogen mode, power mode and polygeneration mode) are investigated. The off-design analysis shows that full integration of the steam cycle between the chemical and the combined cycle islands entails a strong reduction in the plant turndown ratio and significant efficiency losses, so that it is not a preferred solution by the point of view of flexibility. However, it may keep advantages of a shorter startup time and lower capital costs thanks to the presence of a single steam turbine.

From the economic analysis, it resulted that the FTR shows higher competitivity than the ATR if operated primarily in hydrogen mode, while the ATR appears the preferable technology if operated mainly in power mode.

CONFLICTS OF INTEREST STATEMENT

The authors declare the following potential conflicts of interests: S.B. and L.O. are employees of Edison S.p.A., energy utility company operating in the supply, production and sale of electric power and natural gas; M.T. is employee of Ansaldo Energia S.p.A., power generation company manufacturing power plants and equipment (gas & steam turbines, generators and microturbines).

NOMENCLATURE

ASU	Air separation unit
ATR	Auto-thermal reformer
CCS	Carbon capture and storage
CHP	Combined heat and power
FTR	Fired tubular reformer
GT	Gas turbine
HPT/IPT/LPT	High/Intermediate/Low pressure turbine
HRSG	Heat recovery steam generator
IC	Inter-cooled
IRR	Internal rate of return
MDEA	Methyl diethanolamine
NG	Natural gas
S/C	Steam to carbon ratio
SC	Steam cycle
SMR	Steam methane reforming
TCR	Total capital requirements
TIT	Turbine inlet temperature
TOT	Turbine outlet temperature
TPC	Total plant cost
WGS	Water gas shift

REFERENCES

[1] IETA, November 15, 2021, "COP26," Summary report.

[2] Rogelj, J., Shindell, D., Jiang, K., Fifita, S., Forster, P., Ginzburg, V., Handa, C., et al., 2018, "2018: Mitigation Pathways Compatible with 1.5°C in the Context of Sustainable Development," in Global Warming of 1.5°C. An IPCC Special Report on the impacts of global warming of 1.5°C above pre-industrial levels and related global greenhouse gas emission pathways, in the context of strengthening the global response to the threat of climate change" eds., Masson-Delmotte.

[3] Abánades, A., 2018, "Natural Gas Decarbonization as Tool for Greenhouse Gases Emission Control," Front. Energy Res., 6 (47), pp 1-7, doi:10.3389/fenrg.2018.00047.

[4] Taibi, E., Nikolakakis, T., Gutierrez, L., and Fernandez, C., 2018, "Power system flexibility for the energy transition: Part 1 overview for policy makers," IRENA, Renewable Energy Agency, International.

[5] Welch, M., July 15–18, 2019. "Decarbonizing Power Generation Through the Use of Hydrogen As a Gas Turbine Fuel," ASME 2019 Power Conference. Salt Lake City, Utah, USA. doi:https://doi.org/10.111.

[6] Rubin, E.S., and Zhai, H., 2012. "The Cost of Carbon Capture and Storage for Natural Gas Combined Cycle Power Plants," Environ. Sci. Technol., 46, pp 3076−3084. doi:dx.doi.org/10.1021/es204514f |.

[7] ZEP. 2021. "The crucial role of low carbon hydrogen production to achieve Europe's climate ambition: A technical assessment," Brussels, Belgium.

[8] Bauer, C., Treyer, K., Antonini, C., Bergerson, J., Gazzani, M., Gencer, E., Gibbins, J., et al. 2021. "On the climate impacts of blue hydrogen," Sustainable Energy Fuels., 6, pp 66-75, doi:10.1039/d1se01508g

[9] IEA, 2021, "Hydrogen," Paris, IEA, doi:https://www.iea.org/reports/hydrogen

[10] IEAGHG. 2017. "Reference data and supporting literature Reviews for SMR Based Hydrogen Production with CCS," Technical report, TR3.

[11] Dybkjær, I., Rostrup-Nielsen, T., and Aasberg-Petersen, K., 2006. "Synthesis gas and hydrogen," Encyclopaedia of Hydrocarbons Refining and petrochemicals, Volume 2, Beccari, M., and Romano, U., eds., ENI, pp 469-487.

[12] Rostrup-Nielsen, J. R., and Rostrup-Nielsen, T., 2007, "Large-scale Hydrogen Production," Report based on keynote lecture presented at the 6th World Congr. of Chemical Engineering, Melbourne Australia 2001., Haldor Topsoe, p 13.

[13] Aasberg-Petersen, K., Dybkjær, I., Ovesen, C. V., Schjødt, N. C., Sehested, J., and Thomsen, S. G., 2011. "Natural gas to synthesis gas e Catalysts and catalytic processes," Journal of Natural Gas Science and Engineering, 3, pp 423-459, doi: https://doi.org/10.1016/j.jngse.2011.03.004.

[14] Voldsund, M., Jordal, K., and Anantharaman, R., 2016, "Hydrogen production with CO2 capture," International Journal of Hydrogen Energy, 41 (9), pp 4969-4992, doi: doi.org/10.1016/j.ijhydene.2016.01.009

[15] Romano, M. C., Chiesa, P., and Lozza, G., 2010. "Pre-combustion CO2 capture from natural gas power plants, with ATR and MDEA processes," International Journal of Greenhouse Gas Control 4 (5), pp 785-797, doi: https://doi.org/10.1016/j.ijggc.2010.04.015

[16] Moioli, S, Pellegrini, L. A., Romano, M. C., and Giuffrida, A., 2017. "Pre-combustion CO2 removal in IGCC plant by MDEA scrubbing: modifications to the process flowsheet for energy saving," Energy Procedia (114), pp 2136-2145, doi: https://doi.org/10.1016/j.egypro.2017.03.1349

[17] Meissner, R. E., and Wagner, U., 1983. "Low-energy process recovers CO2," Oil Gas J. (81), pp 55–58

[18] DOE/NETL, August 30, 2010, "Assessment of Hydrogen Production with CO2 Capture Volume 1: Baseline State-ofthe-Art Plants," Technical report, National Energy Technology Laboratory, url:www.netl.doe.gov.

[19] Tagliabue, M., and Delnero, G., 2008. "Optimization of a hydrogen purification system," Int J Hydrogen Energy, 33 (13), pp 3496–3498, doi: https://doi.org/10.1016/j.ijhydene.2008.04.055

[20] Yang, S. I., Choi, D. Y., Jang, S. C., Kim, S. H., and Choi, D. K., 2008. "Hydrogen separation by multi-bed pressure swing adsorption of synthesis gas," Adsorption, 14 (4-5): pp 583-590, doi: https://doi.org/10.1007/s10450-008-9133-x.

[21] Aspentech, 2017, "Aspen Plus User Models," Bedford, MA, USA: Aspen Technology, Inc

[22] Renon, H., and Prausnitz J. M., 1968. "Local compositions in thermodynamics excess functions for liquid mixtures," AIChE j., 14, pp 135-144, doi: https://doi.org/10.1002/aic.690140124.

[23] Redlich, O., and Kwong, J. N., 1949. "On the thermodynamics of solutions. An equation of state. Fugacities of gaseous solutions," *Chem. Rev.*, 44(1) ,pp 233-244, doi: https://doi.org/10.1021/cr60137a013.

[24] Chiesa, P., Consonni, S., Lozza, G., and Macchi, E., May 1993, "Predicting the Ultimate Performance of Advanced Power Cycles Based on Very High Temperature Gas Turbine Engines," ASME paper 93-GT-223, doi: https://doi.org/10.1115/93-GT-223.

[25] Chiesa, P., and Macchi, E., 2004. "A thermodynamic analysis of different options to break 60% electric efficiency in combined cycle power plants," J. Eng. Gas Turbines Power 126 (4), pp 770-771, doi: https://doi.org/10.1115/1.1771684.

[26] Chiesa, P., Lozza, G., and Mazzocchi, L., 2005. "Using Hydrogen as Gas Turbine Fuel," J. Eng. Gas Turb. Power 127 (1), pp 73–80, doi:https://doi.org/10.1115/GT2003-38205.

[27] Macchi, E., and Perdichizzi, A., 1977, "Theoretical prediction of the off-design performance of axial-flow turbines." Proceedings of XXXII ATI National Meeting Vol. II, pp 1867–1896.

[28] Giostri, A., Saccilotto, C., Macchi, E., and Manzolini, G., 2012, "A numerical model for off-design performance calculation of parabolic trough based power plants," J. Solar Energy Eng. ASME, 134 (1), doi:10.1115/1.4005105.

[29] Carrara, A., Perdichizzi, A., and Barigozzi, G., 2010, "Simulation of an hydrogen production steam reforming industrial plant for energetic performance prediction," International Journal of Hydrogen Energy, 35, pp 3499-3508, doi: https://doi.org/10.1016/j.ijhydene.2009.12.156.

[30] Campanari, S., Chiesa, P., and Manzolini, G., 2010, "CO2 capture from combined cycles integrated with Molten Carbonate Fuel Cells," International Journal of Greenhouse Gas Control, 4 (3), pp 441-451, doi: https://doi.org/10.1016/j.ijggc.2009.11.007.

[31] IEAGHG. February, 2017, "Techno-Economic Evaluation of SMR Based Standalone (Merchant) Plant with CCS," Technical report.

[32] Lewis, E., McNaul, S., Jamieson, M., Henriksen, M. S., Scott Matthews, S., White, J., Walsh, L., et al. 2022. "Comparison of commercial, state-of-the-art, fossil-based hydrogen production technologies," DOE/NETL, National Energy Technology Laboratory (NETL), Report No. DOE/NETL-2022/3241 doi:https://doi.org/10.2172/1862910.

[33] Chemical Engineering, [Online]. Available: https://www.chemengonline.com/2020-chemical-engineering-plant-cost-index-annual-average/.